minerals

MDPI

Article

Fracture Analysis of α-Quartz Crystals Subjected to Shear Stress

Giovanni Martinelli [1,2,3,*], Paolo Plescia [4], Emanuela Tempesta [4], Enrico Paris [5] and Francesco Gallucci [5]

1 INGV Istituto Nazionale di Geofisica e Vulcanologia, Via Ugo La Malfa 153, 90146 Palermo, Italy
2 Northwest Institute of Eco-Environment and Resources, Chinese Academy of Sciences, Lanzhou 730000, China
3 Key Laboratory of Petroleum Resources, Lanzhou 730000, China
4 CNR-IGAG, Institute of Environmental Geology and Geoengineering, Research area of Rome-1, 00015 Monterotondo, Italy; ilplescia@gmail.com (P.P.); emanuela.tempesta@igag.cnr.it (E.T.)
5 CREA-ING, Consiglio per la Ricerca in Agricoltura e l'Analisi dell'Economia Agraria, Unità di Ricerca per l'Ingegneria Agraria, 00015 Monterotondo, Italy; enrico.paris@crea.gov.it (E.P.); francesco.gallucci@crea.gov.it (F.G.)
* Correspondence: giovanni.martinelli15@gmail.com

Received: 18 July 2020; Accepted: 29 September 2020; Published: 30 September 2020

Abstract: This study assesses the correlations between the intensity of stress undergone by crystals and the morphological characteristics of particles and fracturing products. The effects of the fractures on the microstructure of quartz are also studied. Alpha quartz, subjected to shear stress, is quickly crushed according to a fracturing sequence, with a total fracture length that is correlated to the stress rate. The shear stress generates a sequence of macro and microstructural events, in particular localized melting phenomena, never highlighted before on quartz and the formation of different polymorphs, such as cristobalite and tridymite together with amorphous silica.

Keywords: quartz; shear stress; tribochemistry; fracturing

1. Introduction

The possibility that fractured quartz turns into cristobalite and tridymite poses serious problems in the safe management of industrial milling. In the last twenty years, numerous laboratories have sprung up all over the world conducting experiments on rocks in the conditions of friction typical of technologies utilized in rock grinding. To a large extent, these experiments are carried out trying to correlate the friction coefficient with stress (tangential and normal), the speed and the spaces covered by the simulated fault [1,2]. At the same time, attention has grown towards the "dynamometamorphic" phenomena suffered by rocks and linked to stress: heating, gas dissociation, partial or total melting of the friction layers. In the recent past, several working groups have focused their attention on the role of quartz in the sliding phenomena of rocks, and the idea is that the heating of the contact surface by friction produces a partial melting of the material, the formation of a silica layer amorphous which is quickly hydrated by ambient moisture, which thus becomes a lubricating gel that drastically reduces the friction coefficient of the defects [3,4]. In a recent publication, we formulated another hypothesis to explain the lowering of the coefficient of friction in experiments on quartz-containing rocks. This hypothesis is based on the progressive formation of nanocrystalline cristobalite, which works as a solid lubricant [5,6]. The silica polymorph called cristobalite has the particularity of being an auxetic material, i.e., with a negative Poisson ratio, both in the form of low temperature (alpha) and in that of high temperature (beta). If a layer of cristobalite is found in shear conditions, it can reduce its contact area as a result of the volume contraction and equally reduces the friction coefficient.

The hypothesis is that quartz, subjected to a prolonged reticular distortion over time, tends to take on a structure with ever greater disturbance, but formed by cristobalite nanophases. This phase would be nanocrystalline, not visible by X diffraction but visible by Raman spectroscopy. The accumulation of this phase in the interface between the sliding surfaces would cause the friction coefficient to decay more or less rapidly, depending on the intensity of the dynamometamorphic action [6]. Furthermore, quartz's structural decay is marked by the decay of the electromagnetic signals generated by its fracturing, which diminishes over time as fracturing and damage of the original crystalline structure proceed [5,6]. A key element is missing in this theory: how and when the patina of cristobalite is generated. The purpose of present work is to contribute to a better understanding of the processes related to quartz tribochemistry.

2. Experimental Procedure

The task of this experimental work is to understand the mechanisms that link the progressive demolition of the crystal structure of quartz and the appearance of polymorphic phases during the application of sliding stresses. In two previous works [5,6], the authors of this work reported details on the polymorphic phases of silica that are formed during fracturing and on the correlations between fractures and the amount of very low frequency electromagnetic energy emitted by the crystals during the fracturing.

An innovative "piston cylinder" was used to carry out these studies. It is equipped with two steel pistons which compress the sample and which represent the armatures of a condenser, equipped with an insulating Teflon jacket, which allows the containment of the material. Thanks to Teflon, the pressure distribution exerted is anisotropic, and this is due to the materials that make up the cell itself. The materials that exert the pressure (stainless steel) and the containment material (Teflon) are different in terms of elasticity, coefficient of Poisson and compressive strength. This determines a condition of anisotropy in the exercise of compression: the mineral is not subjected to equal stresses in all directions, but greater according to the direction of the piston and less in the directions perpendicular to it. This anisotropy allows one to create a fracturing system by shear, which generates fractures favoring the development of a network of microcracks. The entire piston cylinder is first evacuated and subsequently subjected to an analytical grade nitrogen flow to ensure an anhydrous atmosphere. The system was created taking into account similar systems published in the past by various authors [7–10]. The pressure is applied through a motorized hydraulic press, which develops a maximum load of 4.9 kN.

The quartz-α samples come from natural quartz crystals, purchased at Ward (Ward, West Henrietta, NY, USA; www.wardsci.com), previously analyzed in optical microscopy to detect any defects, such as inclusions and fractures. The crystals were chosen in the weight range from 0.05 to 1.5 g. Each test generated powders and fragments that were analyzed for shape, size, area and volume, through the new Morphology G3ID image analysis system (Malvern, UK) based on optical scanning microscopy. The automated scanning system allows one to measure and analyze about 1 million particles per hour and to know the values of the perimeter, area and volume of each particle, from 300 µm to 1 µm. This scanning microscope has already been used previously by the authors for investigations on asbestos fibers in soils and recently on quartz crystals [5,6]. To determine the morphologies, the particles are dispersed on the surface of the optical plate. Scanning takes place at constant magnification on all particles following an *x*-*y* scanning mechanism; the depth of the particles is reconstructed through the "*z*-stacking" mechanism that allows one to shoot the same image of the particle on different focal planes.

In this work, we used the data of the optical scan to estimate the quantities of "new" surfaces generated by the fracture, the statistics on morphologies (equivalent diameter, area for every particle). These data were compared to the entity of the stress rate. The calculation of the real volume deserves special mention. The instrument software measures the volume by the diameter equivalent to the sphere (SE Volume), but this value is very far from reality. Therefore, we used an algorithm that is based on the measurement of the attenuation of the intensity of light transmitted by the particle.

For non-scattering media, the Beer–Lambert law (BL, or absorption law) is well recognized to describe the relationship between transmittance and sample thickness as:

$$T = \exp(-\mu_a d) \quad (1)$$

where T is the transmittance, d is the sample thickness, and μ_a is the absorption coefficient (cm^{-1}). This expression is based on the random nature of stochastic light absorption, characterized by the rate constant μ_a. Since the transmitted light intensity is measured for each particle, and since we are always in the presence of quartz, which has an absorption coefficient from 664 cm^{-1} at 450 nm to 312 cm^{-1} at 650 nm [10], the thickness "d" can be derived for all particles. Figure 1A shows the effect of fracturing on quartz grains; the images have been modified after Zhao, B. et al. [11]. On the left, we can see the two-dimensional projection of the particles obtained from the compression fracturing of a quartz grain. The perimeter of the granule, obtained from the two-dimensional projection, is expressed in green. The perimeters of the projections of the individual particles obtained from the fracturing are indicated in red. In Figure 1B, images of the original crystal, a tip weighing 207 mg and some of the particles obtained from the fracturing can be observed.

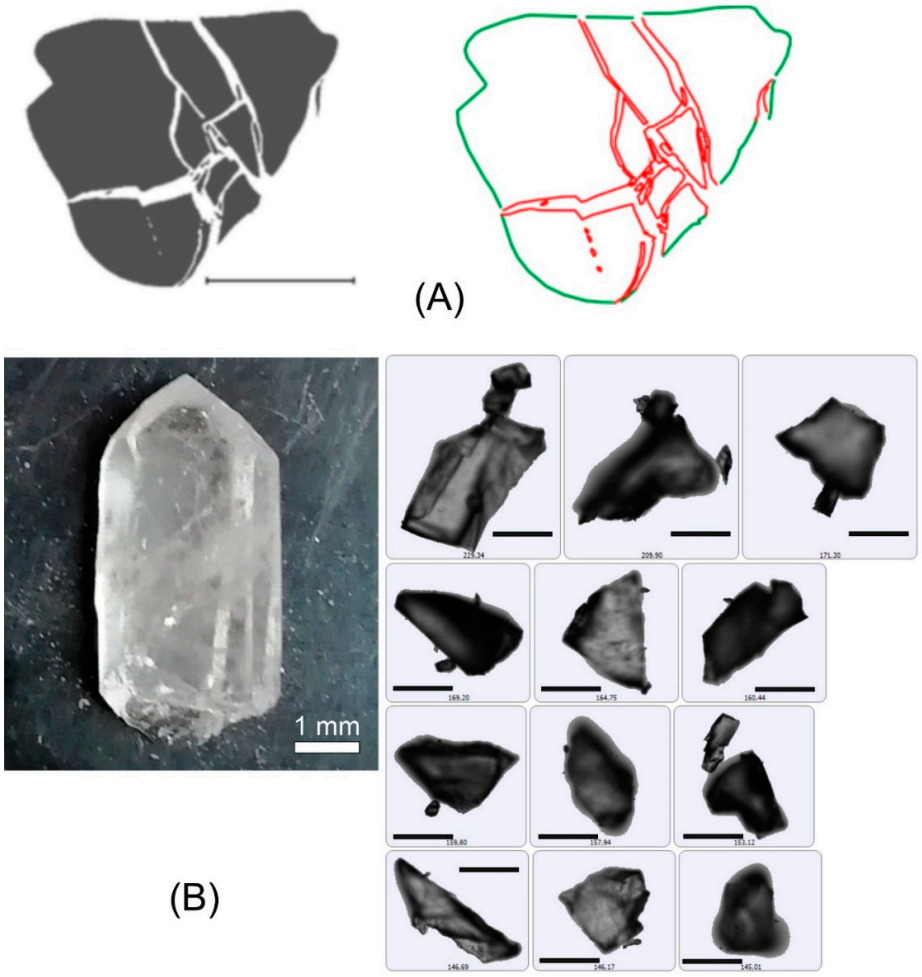

Figure 1. (**A**) Breakage of a grain: on the left, projection images of particles created by the breaking of first grain; on the right, original perimeter (green) and new perimeter (red). (**B**) On the left, the image of the original crystal fragment, 207 mg in weight; on the right, the 12 largest fragments of the left crystal; each fragment of the crystal, from 0.3 mm to 1 µm, was analyzed from the morphological and dimensional point; in total, the left crystal produced over 320,000 fragments; the black barindicates 150 µm.

The surfaces of the "internal" granules are, in fact, the new fracture surfaces, created when the imposed stress exceeds the critical stress level. The sum of the surfaces of the particles will be equivalent to the sum of the new surfaces created by the fractures, S_{tot}, plus the original surface. In this way, it is possible to calculate the total area created by the fractures. By extrapolating this concept, it is also possible to calculate the total length of the fractures. The total perimeter of all particles is correlated with the total length of the fractures, minus the original perimeter of the crystal and the loss of data due to the two-dimensional transposition of the three-dimensional particles. The latter error is reduced if the particles analyzed by microscopy are in very large numbers. For this reason, the analyses in morphology must be carried out on a high number of particles, usually above 100,000 particles.

In order to determine the nature of silica polymorphs, a Raman microprobe inserted in the Morphology G3ID was used, which uses a 785 nm laser with a spot of 2 microns in diameter. The Raman laser power is 40 mW.

To determine the stress to which the crystal is subjected, a measurement method was developed using the image of the shattered crystal printed on a pressure sensitive film (Pressurex Inc., Madison, NJ, USA; www.sensorprod.com). These films have an ink layer that produces a color, and the intensity of which is proportional to pressure. Figure 2 shows the pressure marks left on the film by different quartz crystals

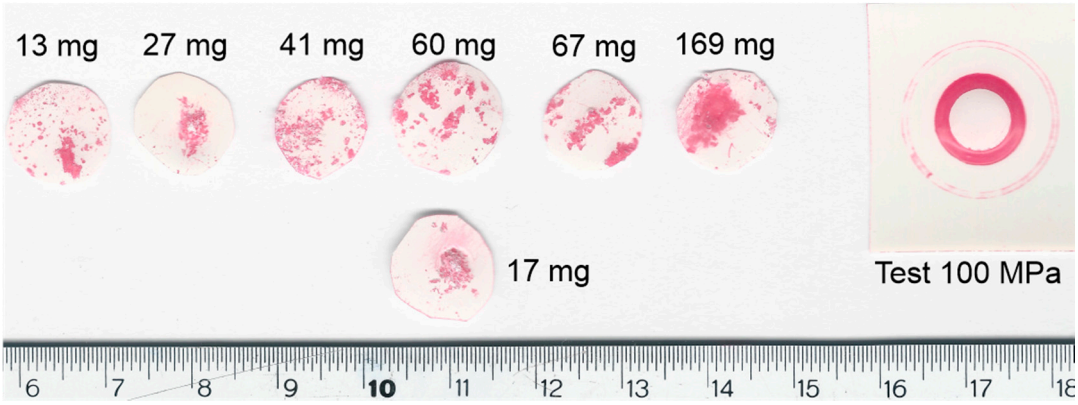

Figure 2. Images of the films impressed by several compressed crystals; on the right, a calibration test. The numbers represent the weight of samples in mg.

Finally, we used scanning electron microscopy to determine the microscopic characteristics of fractures at different stress levels (Zeiss EVO MA10, Zeiss Gmbh, Ulm, Germany). The samples to be analyzed in the SEM were left in their original condition, without cleaning, since debris on the surfaces of the granules can provide important information.

3. Results

3.1. Particle Size Distributions Related to Stress Conditions

The sizes of the quartz particles show complex correlations with pressure undergone and linear correlations between the rate of increase in pressure and the average size.

The particle size curves (Figure 3) obtained from the tests show a distribution of variable shape:

- For particles from samples subjected to a more intense stress rate (MPa·s^{-1}), the distribution is shifted towards the larger particles, and the shape of the curve is monomodal.
- For the particles that have undergone a slower pressure rate, the particles have had time to fracture more, and the distribution is shifted towards smaller particles, with a bimodal curve shape.

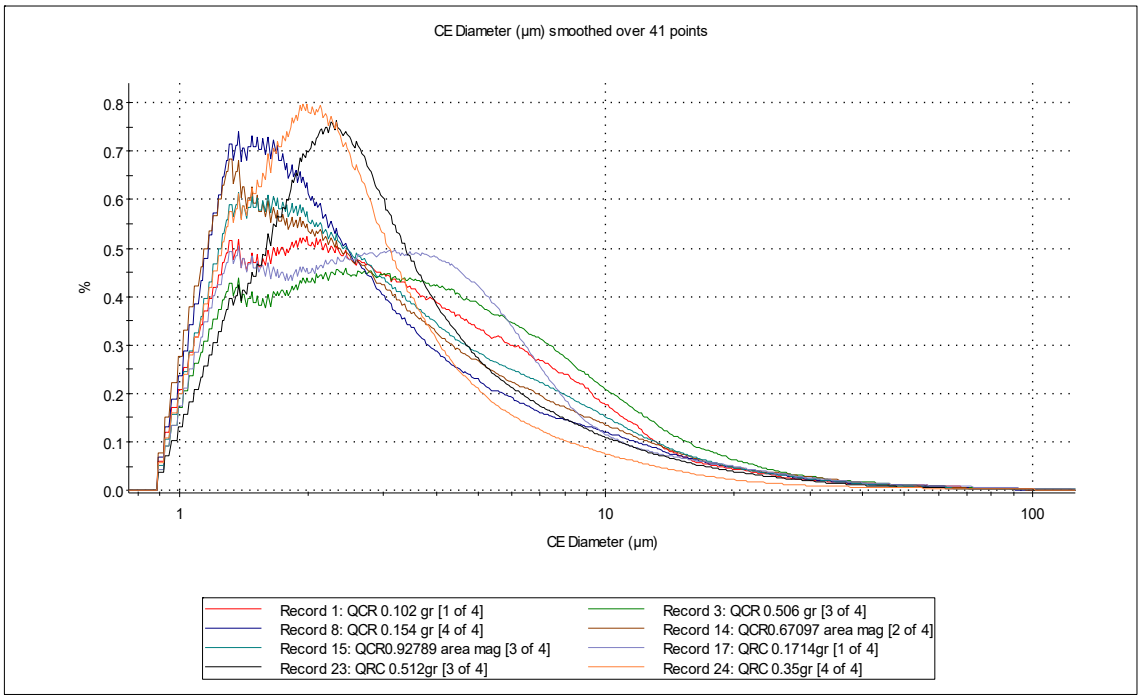

Figure 3. CE diameter distribution curves of quartz particles (the meaning of CE is "circle equivalent"; the curves are obtained from the smoothing by average of 41 readings; the results are expressed in *x*-*y* graphs and not in histograms, due to the high number of reading channels; and gr is the weight of sample, e.g., 0.102 gr as grams, 102 mg).

Figure 4 shows the correlation between the total length of the fractures per unit of quartz weight (calculated on the basis of the total perimeter of the particles) and stress rate.

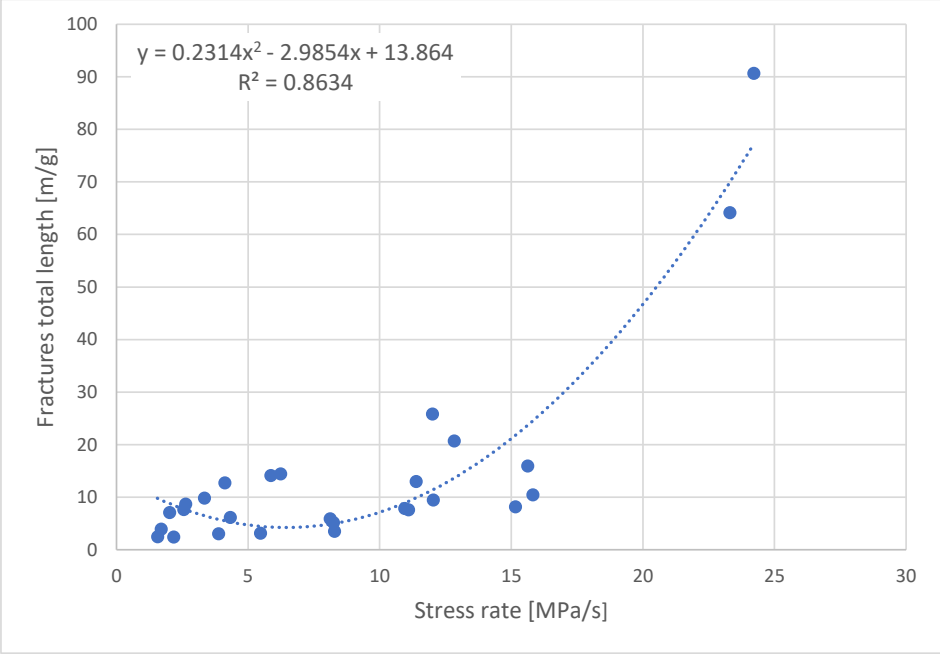

Figure 4. Correlation between the stress rate and total fracture length.

3.2. Determination of the Morphological Characteristics of the Fractures

The morphologies of the fractures in the quartz granules after the cutting effort are extremely varied and interesting, showing that the fracture phenomenon of this mineral is very complex and connected to a large number of parameters. We analyzed the data obtained from the analysis of the images, starting from the samples that underwent the least intense pressures, to end with those that underwent the greatest pressure.

In Figure 5, the fracture forms left on the quartz granules by stress rates of about 0.5 MPa/s are observed. Stress creates a first series of conchoidal-shaped fractures. Around it, there are "sawtooth" shapes of homogeneous dimensions. The average height of the teeth is 2.3 μm. The area filled with these teeth is extremely large and covers several hundred μm^2. We initially thought that these forms were related to a Dauphine twinning; after careful examination we decided not to include this result, as it is still unclear. Dauphine gemination is however compatible with the stress regime to which quartz crystals are subjected in our experiments; in particular, Laughner et al. [12] demonstrated that the stress required to produce twins can be lower than 88 MPa. Since the strength of quartz on compression is 200–300 MPa, Dauphiné twinning generally precedes brittle fracture.

In samples subjected to stress of greater intensity and rate (5–50 Mpa/s), simpler fractures are generated that extend for distances from a few units to a few tens of μm. Figure 6 is a mosaic of eight photos taken on a quartz particles with some ridges and fractures. These fractures (Figure 6) show a profile raised above the surface with a vaguely triangular section and an average length of 20–30 μm from the beginning of the fracture until the first bifurcation, which invariably occurs at angles of 27°. In larger grains, the fractures end with euhedral shaped craters of very variable sizes, from 150 nm to 1–2 μm (Figure 7). The shapes of the craters are regular, with hexagonal, square and trigonal geometries; only the smaller craters are elliptical (Figure 7). Most of these craters are aligned in directions inclined with respect to the direction of the fractures. These alignments reach conspicuous dimensions, often exceeding 100 μm. In some areas, where the density of craters is of the order of one every 2–3 μm, the craters unite and form open fractures, ranging from a few to ten μm wide and proportional lengths of up to 100 μm. In the fragments of the samples subjected to the maximum stress, the presence of "bubbles" is observed on the surface of the material with fractures on the surface (Figure 7C). These bubbles open in some places, forming small craters (50–100 nm), resembling real "hot spots" with a raised edge of apparently melted material (Figure 8). At the apex of some fractures, there are also real "protrusions" (Figure 9), while in rare areas, there are open fractures and craters filled with quartz crystals, that are elongated and small, with diameters of 0.5–0.8 μm and lengths of 1–1.5 μm, and often twinned (Figure 10). The same phenomenon can be observed in some open fractures, completely covered by newly formed quartz crystals, from which the crystals are arranged according to a design that mimics an exit direction of the precursor material. Along the fractures, detachments of filamentous material are observed, starting from the starting point of the fracture (Figure 11). These filaments are composed of silica alone. These fibers are characterized by diameters between 50 and 200 nm and lengths of from a few μm to tens of μm, and they follow the fractures until they detach, and, then, they can take on twisted, curled or meandering shapes. Their section is slightly flattened, almost as if they were ribbons. On the points of the greatest concentration of fractures, hundreds of these filaments are observed, which start from the fractures in a crystallographic direction and then tend to detach (Figure 11).

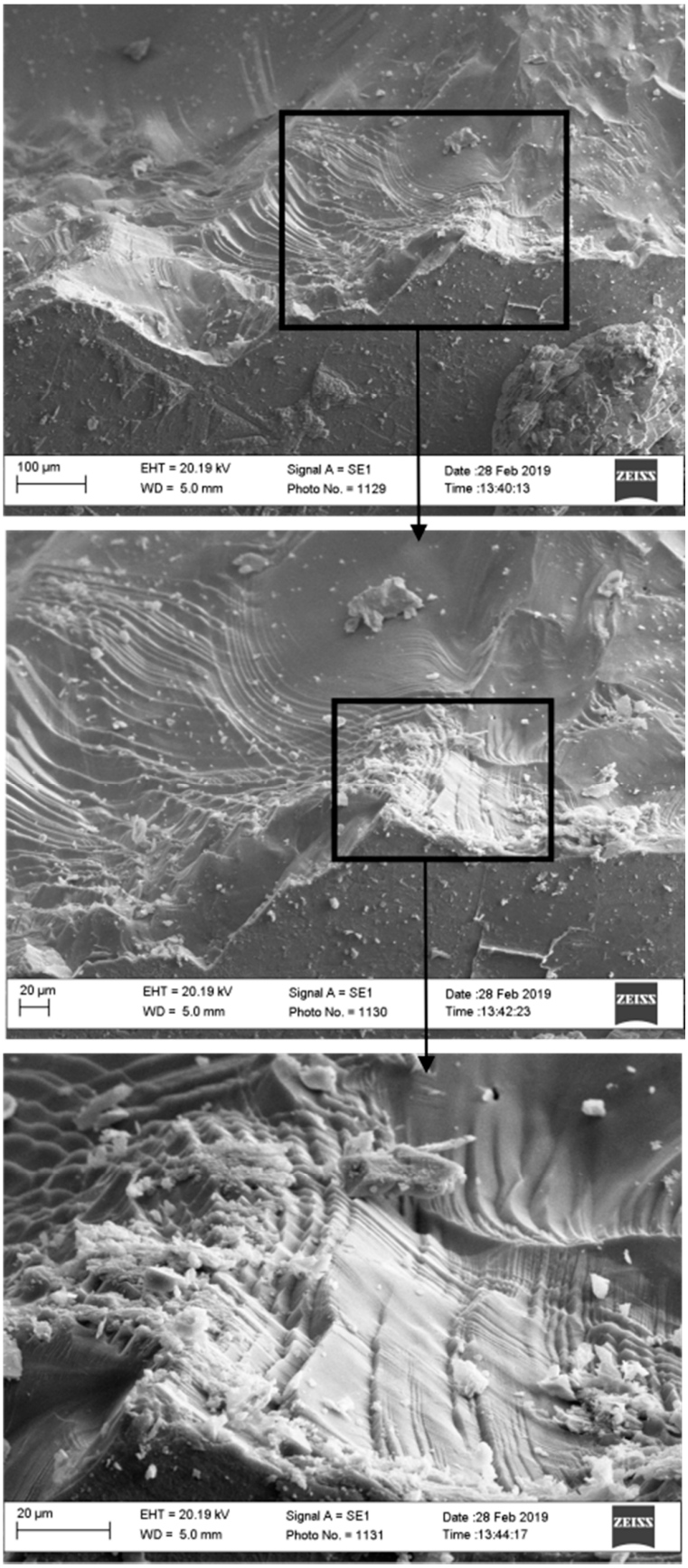

Figure 5. Sawtooth forms generated by the combination of two conchoidal fractures on the surface of the quartz granules; stress rate: 0.5 MPa/s.

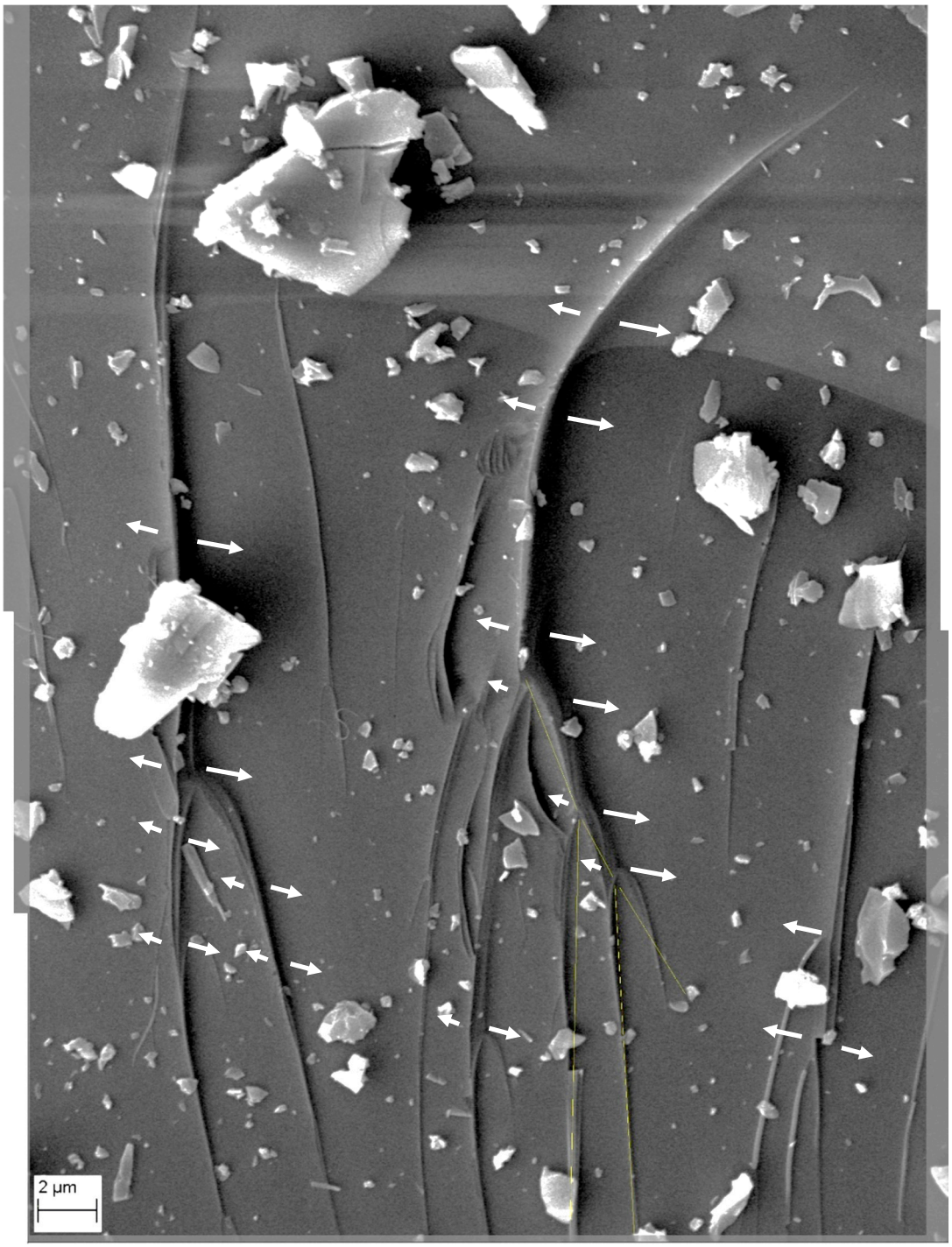

Figure 6. Fractures on the surface of a quartz granule subjected to 100 MPa; the bifurcations show angles of about 27° (taken from the work of Martinelli et al. [5]).

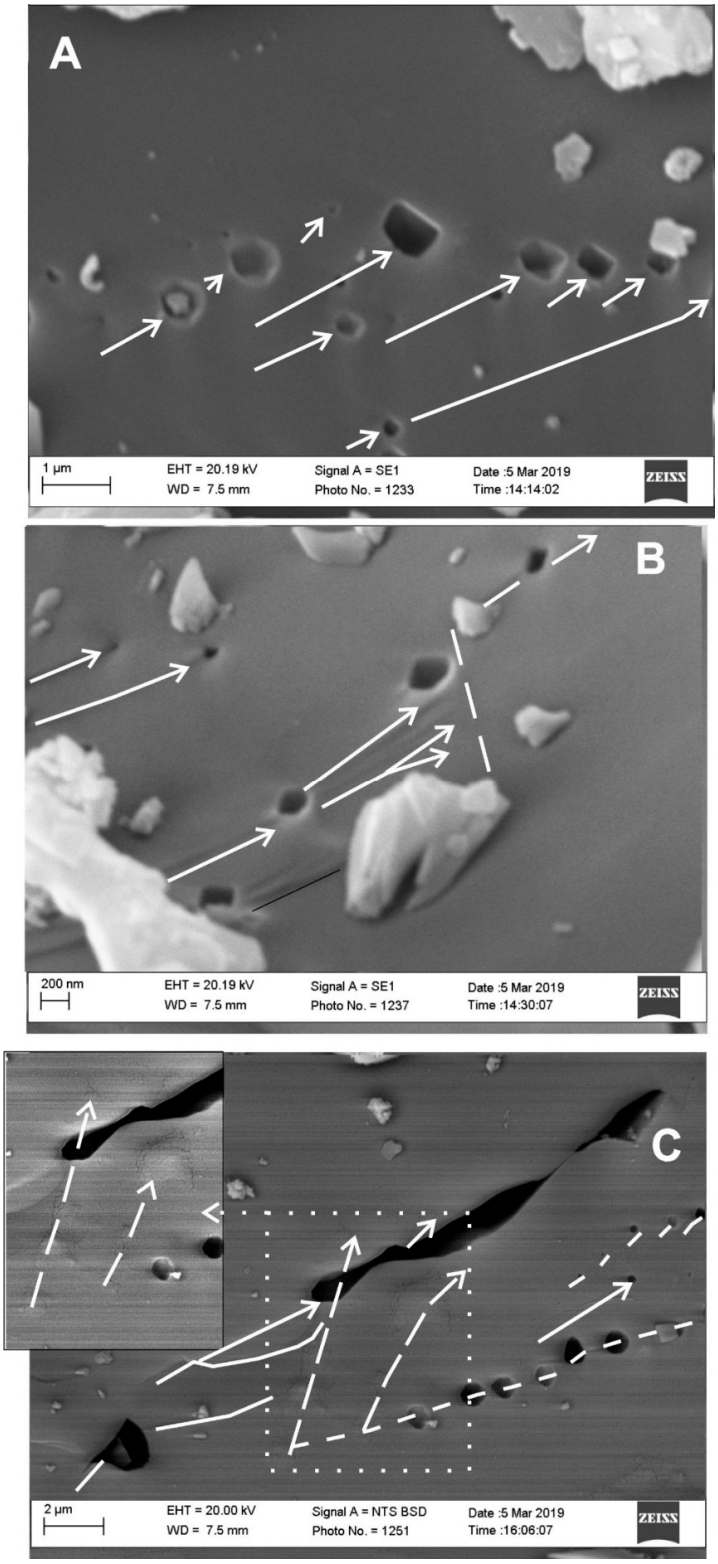

Figure 7. Fractures in the granules at 150–200 MPa; in photo (**A**) the euhedral shapes of the craters at the apex of fractures of a few microns are well observed. Photo (**B**) shows the formation of several generations of fractures starting from the craters. In photo (**C**), there are open fractures formed by the coalescence of the craters that form at the end of the fractures; on the left, aligned bubbles, barely visible on the surface of the granules. In white, the apparent directions taken by the fractures, in black the visible directions.

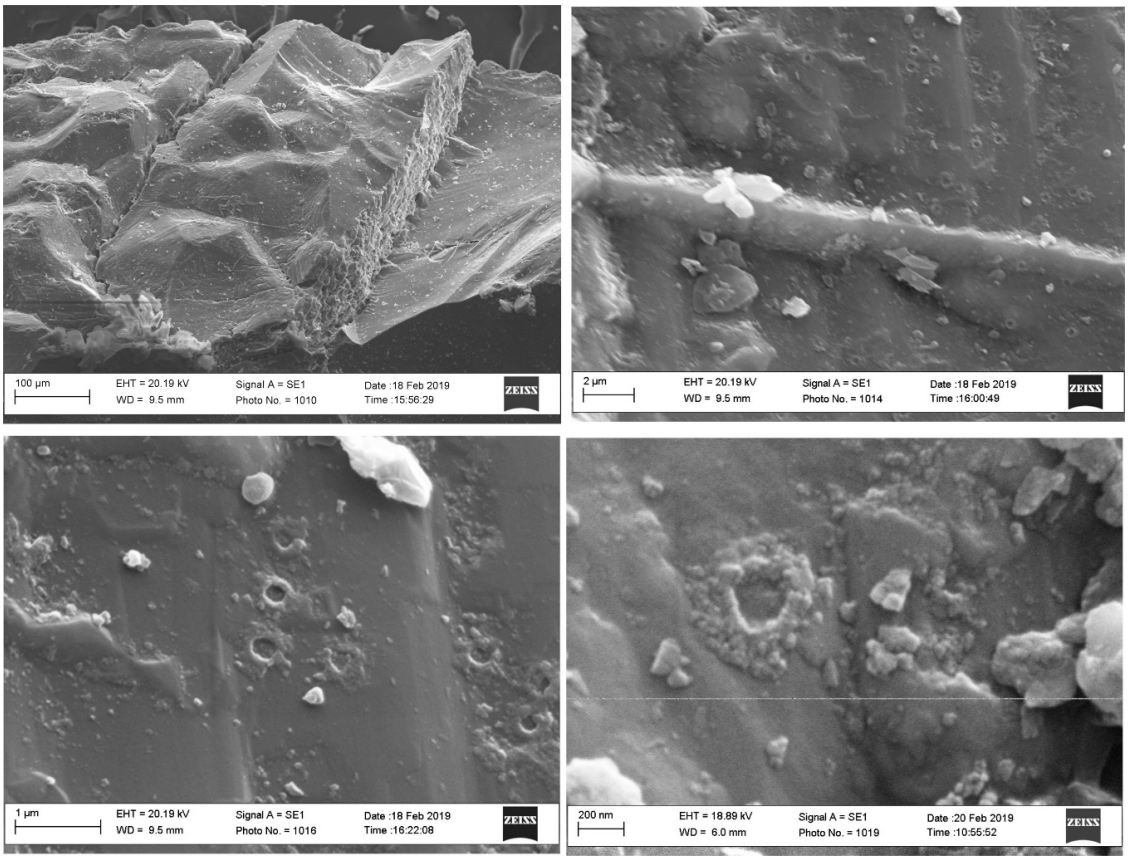

Figure 8. Quartz, 120 MPa: "hot spot" on quartz particle surfaces.

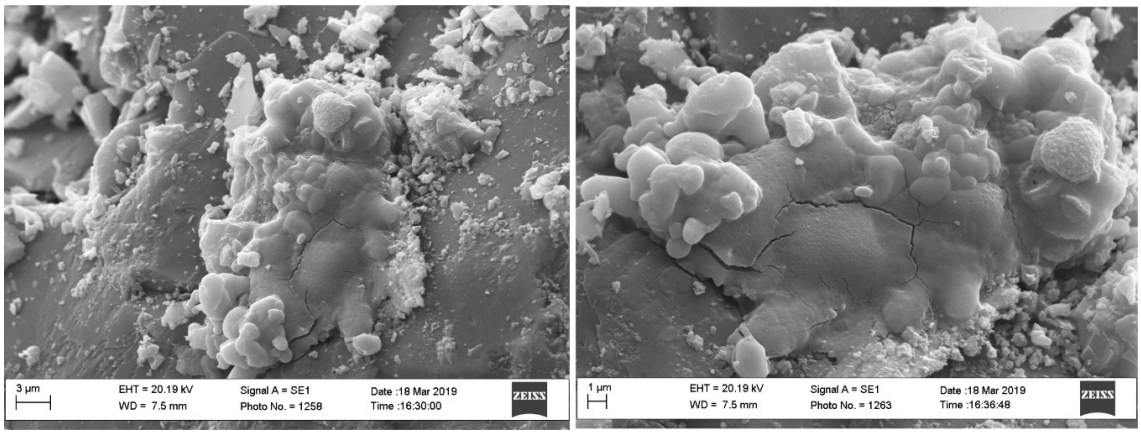

Figure 9. Quartz, 220 MPa: amorphous silica extruded from a fracture on quartz surface.

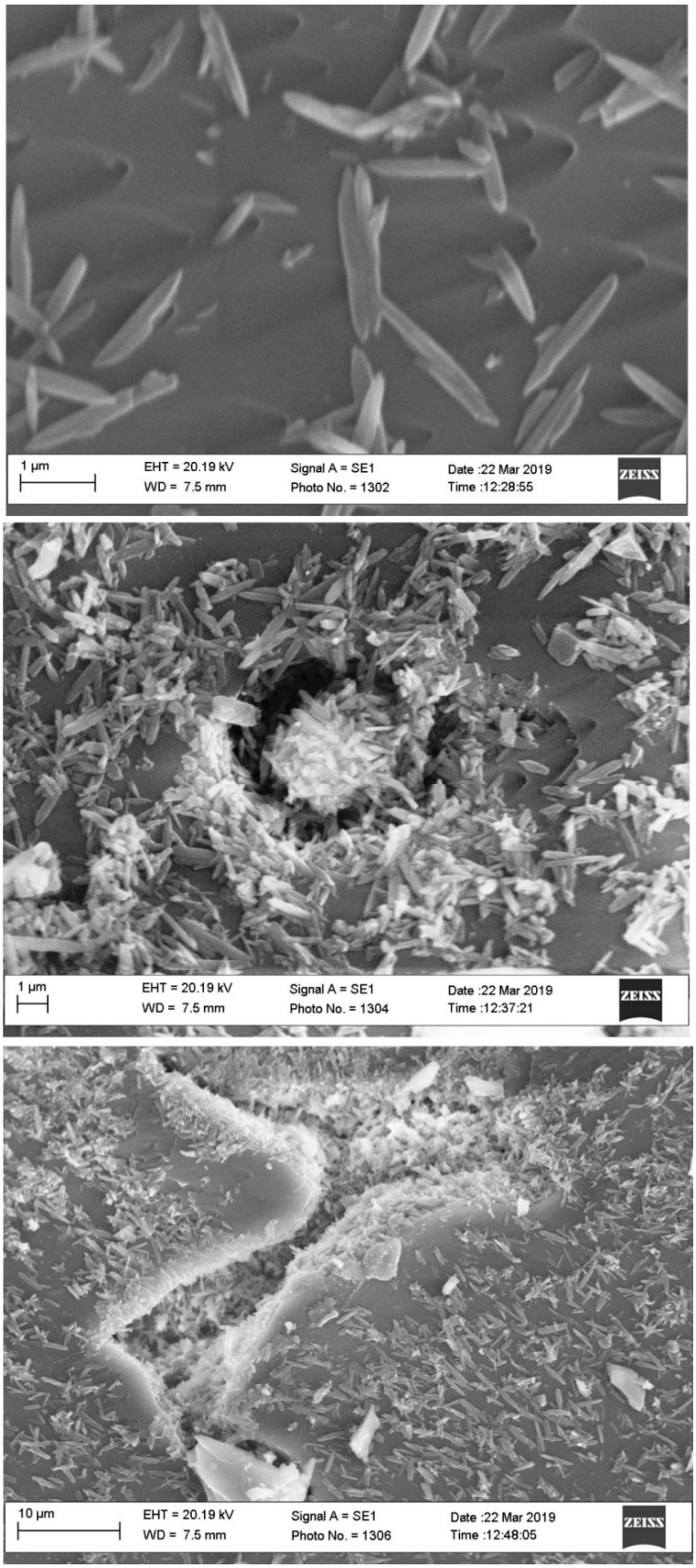

Figure 10. Quartz, 230 MPa: crystallization and growth of quartz microcrystals from silica near fractures and hot spots.

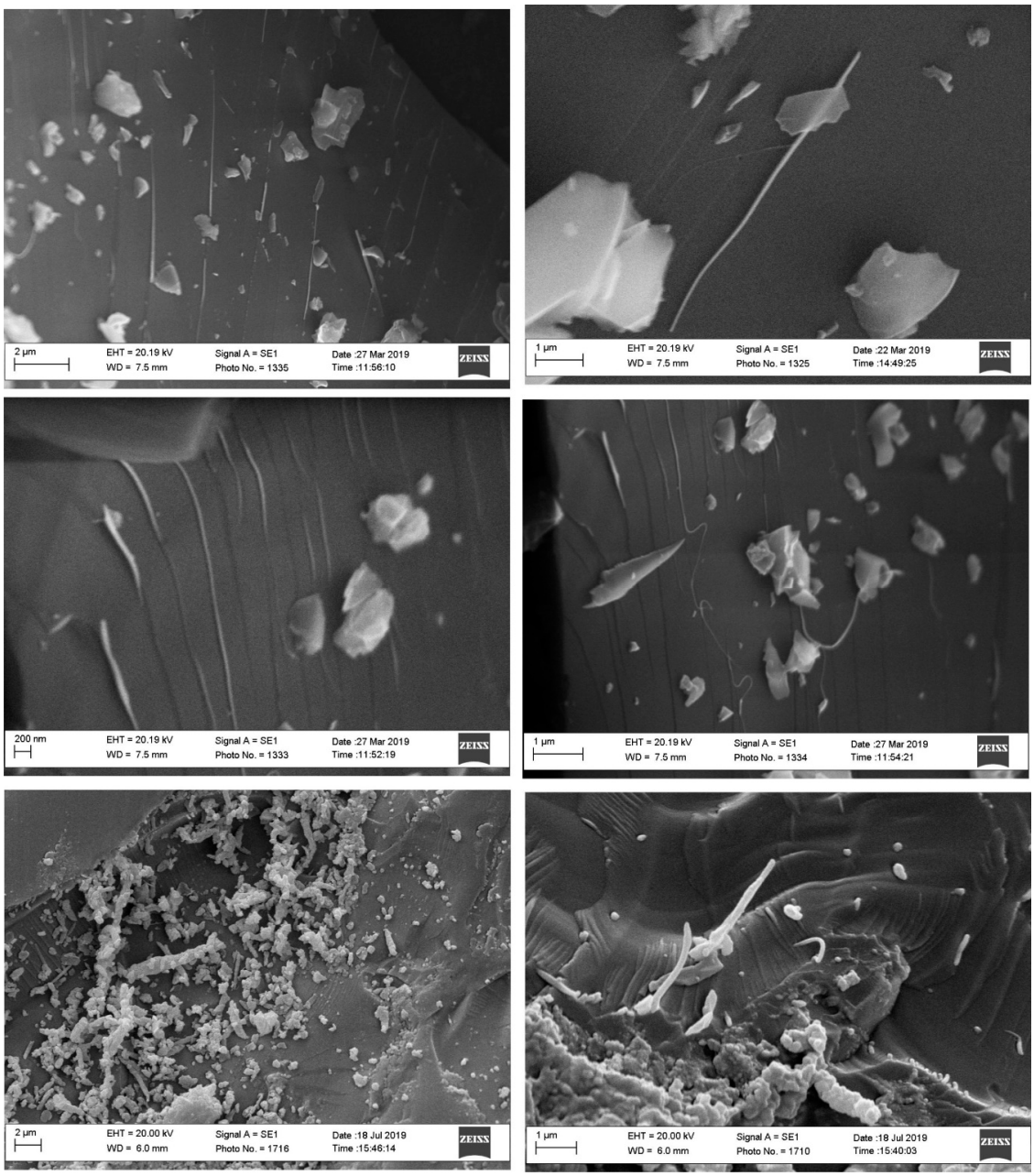

Figure 11. Filamentous forms of silica that are an integral part of fractures of the type shown in Figure 6.

3.3. Raman Analysis of Solid Phases on Fracture Surfaces

Raman analyses were performed on fracture surfaces that appear dark under an optical microscope in polarized light and on areas where fracture streaks with fibrous traces are present. Figure 12 shows some spectra taken respectively in dark isotropic areas. Given the size of the Raman laser spot used (≈2 µm), the analysis cannot select only the filament areas that are smaller than 1/10 of spot, but will also include areas where there is certainly undisturbed quartz. Despite this, the analysis clearly shows the presence of α-cristobalite and tridymite in very variable proportions (Figure 12). In the first spectrum (white) the 465, 404 and 365 cm^{-1} bands of alpha quartz are observed. It belongs to an optically non-isotropic zone. The underlying spectra, indicated as Black1, Black2 and Black3 in Figure 12, are three selected areas within optically isotropic areas of approximately 4 μm^2 each. In the spectra we observe the presence of the most intense bands of quartz, but also of tridymite and cristobalite, albeit of reduced intensity. The identified cristobalite is of the alpha type, while the tridymite is similar to the

PO10 polytype, as per Ruff standard of said mineral. On the right, an enlargement of the spectra is observed in the range of 440 to 320 cm^{-1}. The Black1, 2, 3 spectra have been recorded at 200 Mpa; the quantity of these isotropic patches seems to increase with increasing pressure and with time of stay under stress.

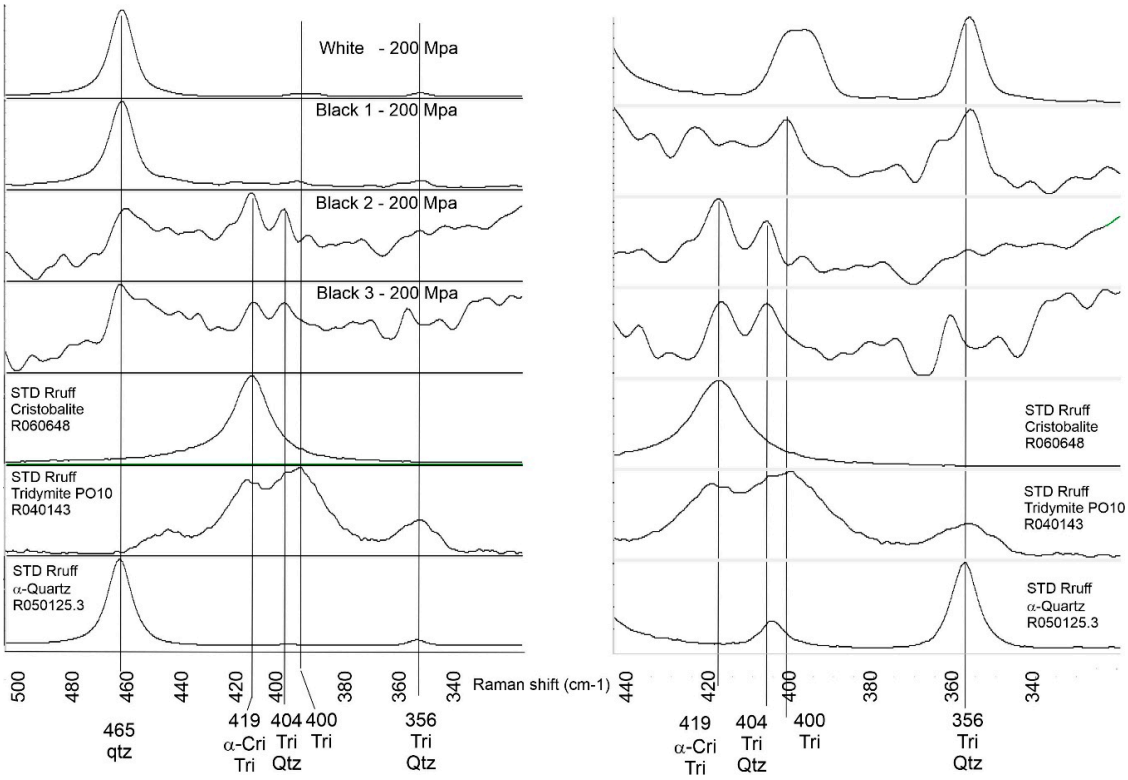

Figure 12. Raman spectra of stressed quartz fragments; the three spectra below derive from the collection of Raman spectra included in the RRUFF collection (RRUFF Project, Department of Geosciences, University of Arizona, 1040 E 4th, Tucson, AZ, USA. 85721-0077): (Cristobalite (low)-R060648, Tridymite PO10-R040143, Quartz (low)-R050125.3); on the right, an enlargement of the area between 440 and 320 cm^{-1}.

4. Discussion of Data

The data obtained in this study should be seen in the light of the most recent literature on the effects of shear stress on alpha quartz, literature to which the authors have also contributed [5,6]. The fractures we have observed show an evolution which, we believe, depends substantially on the stress rate rather than on the pressure itself. In fact, we have verified that even a pressure of 50 MPa, supplied in times exceeding one minute, generates a more intense fragmentation than a pressure of 100 MPa supplied in times of a few tens of seconds. The most relevant phenomena observed on quartz granules that have undergone increasing stress are as follows:

- Formation of craters with euhedral shape at the apex of the fracture;
- Coalescence of the craters to form open fractures;
- Detachment of apparently amorphous siliceous material, fibrous in shape from the ridges and traces of fractures;
- Bubble formation on the surface, some of which show amorphous silica extrusions;
- Formation of craters on the surface from which amorphous silica is expelled;
- Formation of secondary quartz crystallizations, which radiate from "emission" points, such as craters and open fractures.

From Figure 4 it can be observed that the fracture length increases exponentially with the increase in the stress rate. This is reasonable, since the total length is related to the number of particles and this to the number of bifurcations of the cracks that are generated during the breaking of the quartz crystals. Cracks that reach critical speed tend to divide into two cracks (bifurcations) with an acute angle between them, as demonstrated by Tromans and Meech [13–15]. Consequently, if the stress velocity is greater, the cracks' opening speed will also be greater, and this will produce more fractures and a greater number of particles.

In Figure 6, the ridges indicate the presence of fractures under the surface. The crests indicate an increase in volume propagated linearly along the fractures. The fractures separate into two sections with an acute angle of 27°. As is known, the angle of forking varies with the stress state. In particular, the bifurcation angle indicates the relationship between shear stress and normal stress τ/σ_n. An angle of 27° corresponds to a ratio from −0.3 to −0.5, which essentially indicates a bending stress (Richter, 2003) [16]. Both the total length of the fractures and the amplitude of the bifurcation angle are parameters to be framed in a wider context of energy analysis of the fracturing phenomenon, for which the reader is referred to the cited bibliography. In this context, it is sufficient to remember that the fracture length is connected with the fracturing speed [13–15]. The cited authors calculate that in alpha quartz, the fractures split in two when the propagation speed reaches the *climit* (limit speed of 1990 m/s). At that moment, the ratio between the size of the new fracture, a_i and the initial size, a, is equal to 2, and the speeds of the two daughter fractures is reduced to 30–50% of *climit*. The two fractures thus formed increase their speed and must again fork when they reach *climit* and at an a_i/a ratio of 4, according to relation:

$$(a_i/a)_{\text{branch4}} = 2(a_i/a)_{\text{branch3}} = 2(a_i/a)_{\text{branch2}} = 2(a_i/a)_{\text{branch1}} = 2(a_i/a)_{climit}$$

It is important to note that an increase in the propagation speed leads to a higher frequency of bifurcations and therefore to a greater fragmentation. This is confirmed by the observations made with the analysis of the morphological image of the particles, where it is evident that a higher stress rate increases the number of particles and the total fracture length (Figure 4). It is noteworthy that the propagation of fractures in the minerals causes an accumulation of deformation energy, and this energy must dissipate; in mineral mechanics, the ways of disposing of the plastic deformation energy are essentially two: the bifurcation of fractures and, above all, the increase in temperatures in the deformation areas at the fracture tip [17,18].

The formation of the craters visible in Figure 7A–C is consequential to the propagation of fractures. In Figure 7A,B it is observed that the fractures end with a regular-shaped crater, often mimicking a crystalline form with five to six faces. The volume of matter removed from these craters seems independent of the visible (or superficial) length of the fractures. We believe that the loss of fragments of material with crystalline forms is linked to the presence of fracture lines already existing in the crystal, parallel to crystallographic directions. The reader should also note the correspondence between the apex of the fracture and the corresponding crater. We believe this is due to the undermining of the material by the wave at ultrasonic speed connected to the propagation of the fractures. Figure 7C shows the presence of surface bubbles that show cracks of about 40 nm width and lengths of about 1 μm. The bubbles also appear aligned, according to directions that lie at 60° with respect to the fractures. We believe that these bubbles are the superficial manifestation of the melting effect at ultrasonic speed that occurs inside the quartz grains during the crack propagation and which produces most of the phenomena we are describing. The same phenomenon is responsible for the formation of the craters aligned with the amorphous silica extrusions, visible in Figure 8, the silica extrusions in Figure 9, the recrystallized quartz from silica extrusion in Figure 10 and, finally, the filamentous fibers in Figure 11 that are, perhaps, the most interesting part of the discoveries made in this work. The Raman analysis performed on the silica fibers associated with the fractures shows that this silica is organized in the form of α-cristobalite and tridymite (Figure 12). The presence of cristobalite had already been highlighted by the authors of this work [5,6], where the structural changes of quartz in

nanocrystalline cristobalite were described when alpha quartz was subjected to shear stresses. In the aforementioned work, we have shown that the action of prolonged shear stress on the quartz crystals determines a reticular distortion so large as to lead the quartz itself to an amorphization; in this "amorphous silica", the radial distribution function analysis (RDF) has highlighted the formation of short-term clusters with a six-tetrahedron organization, similar to cristobalite and tridymite and no longer to four tetrahedrons [6]. It has also been shown that, if these amorphous phases are brought to 1200 °C, they tend to transform nano-cristobalite into a well-crystallized cristobalite, well visible in X-ray diffraction analysis [6]. The same association of minerals had been reported in a paper of Brodie and Rutter (2000) on quartz samples subjected first to tensile stress and then to heating at 1200 °C [17].

To explain the data collected, we hypothesized a mechanism that can materialize thanks to the speed of propagation of the fractures. The heart of the mechanism is tensile stress, which induces the opening of a large number of fractures in the quartz volume. Fracture propagation occurs at an estimated speed between 50% and 60% of the shear wave, therefore between 650 and 1000 m/s, and for this reason we can speak of ultrasonic speed. At these speeds, the fractures tend to fork after just 25–30 μm, and the crack tip transit times are therefore in the order of 30 ÷ 50ns. In such a short fraction of time, the amount of heat produced by the passage of the crack tip cannot have transferred to the volume outside the fracture. Weichert had already measured temperatures above 2000 K on the fractured quartz, and this has been confirmed by other authors [18,19]. These temperature increases generate channels of fused silica, which has a decidedly lower density than quartz (2.2 g/cm^3 against 2.65 g/cm^3). The decrease in density causes an immediate expansion in volume which causes surface fracturing. In actual fact, we can say that during the melting, the molar volume increases from 22.688 cm^3/mol to 27.20 cm^3/mol, with an expansion of 16.5% [19], more than enough to open the surface over the crack and bring out the fused and clotted silica filament that is inside it.

The events we have described are summarized in the diagrams in Figure 13. In the first one, we observe the simulation of the silica filaments growth, starting from the fractures; Figure 13B shows the formation of fractures ending with the euhedral craters and the formation of bullous-shaped growths. Figure 13C shows the pattern of crater formation ("hot spot") and silica protrusion from subsurface melted areas. Our data demonstrate that the friction action applied to quartz in totally anhydrous conditions leads to the formation of amorphous silica, which quickly organizes itself into nanostructures of cristobalite and tridymite [5,6]. Cristobalite has a structure consisting of rings with 6 tetrahedra, with structural arrangements that show an auxetic behavior, that is, with a negative Poisson's ratio [20,21] (Table 1). This means that a tangential compression produces a reduction in length in the normal direction and not an expansion, as expected from solids with a positive Poisson's ratio. The effect is particularly felt by the alpha cristobalite, whose Poisson ratio reaches the considerable negative value of −0.169. In practice, if the tangential contraction is 100 mm, the normal contraction will be 16.9 mm; this reduces the contact surface and correspondingly reduces its friction. It should also be taken into account that the phenomena whose generation we have verified are extremely fast, because they occur in the time interval that elapses during the final phase of propagation of the fractures. The speed of these contractions is linked to the propagation speed of the ultrasonic wave.

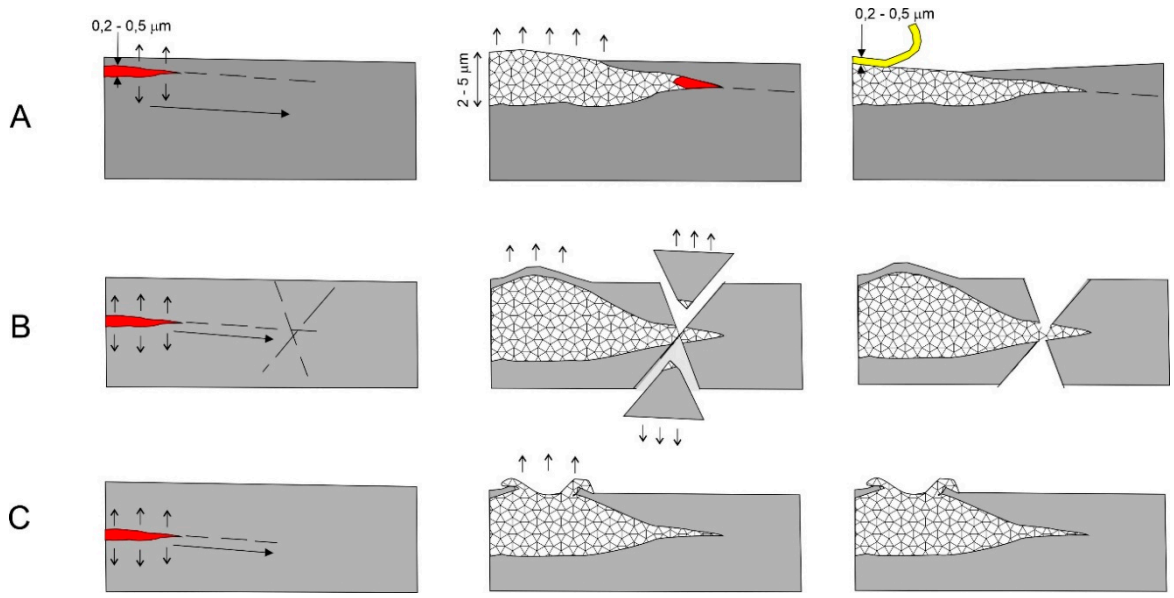

Figure 13. Scheme of propagation of fractures in quartz granules; (**A**) beginning of the phenomenon, as the fractures spread; (**B**) formation of fractures ending with the euhedral craters and superficial "elevations"; (**C**) formation of craters ("hot spots") and the protrusion of silica from the molten areas below.

Table 1. Mechanical parameters for silica polymorphs [13,14,20], G = Shear modulus, E = Young modulus, n = Poisson ratio, ϱ = density, ε = strain.

Silica Polymorphs	G	E	υ	ϱ	ε
	Gpa	Gpa	n	g/cm^3	%
quartz alpha	44.1	95.6	0.084	2.65	8.4
quartz beta	41.5	99.1	0.194	2.53	19.4
cristobalite alpha	37.1	61.3	−0.169	2.32	−16.9
cristobalite beta	32.6	62.3	−0.044	2.20	−4.4
tridymite low	28.8	58.1	0.004	2.27	0.4
tridymite high	26.7	52.8	−0.011	2.26	−1.1
Silica glass	33.4	79.3	0.187	2.20	18.7

If the application of stress is continuous, there is an accumulation of amorphous silica that quickly transforms into cristobalite and tridymite near the fracture and sliding areas. The mechanisms described also explain the so-called "flash melting" which is observed by numerous authors in the shear stress tests on quartz and, above all, the sudden drop in the coefficient of friction that all the authors observe when the quartz is subjected to severe friction conditions [1]. Various authors support the thesis that the friction, exerted on quartz-rich rocks, generates a sort of silica gel lubricating film, an amorphous material rich in water, deriving from the environment where the test takes place. The concept of the lubricating gel is also taken up by [4], who had detected the presence of amorphous silica in the flow tracks of experiments by means of tribometric rotating friction apparatuses, such as the "pin-on-disk" on quartz [3,4]. Authors detected, via Raman spectroscopy, the peaks attributable to moganite (metastable phase of silica, quickly converted into cristobalite and tridymite) and to amorphous silica, as well as reticular distortions of alpha quartz. In addition, the authors showed spectra in FTIR microspectrophotometry to prove the presence of water in the amorphous silica of these traces of flow. The results obtained, albeit preliminary, do appear interesting. In particular, the fact that amorphous silica has hydrated with atmospheric humidity is possible, but it does not prove that it is the means of sliding the faults that insist on quartz-based rocks. In our tests, carried out under anhydrous conditions, there can be no water presence, but the same amorphous silica and cristobalite

and nanocrystalline tridymite are formed, which, as we have said, have the characteristic of reacting to efforts by decreasing the contact area, with relative reduction of the friction coefficient. At the end of this long discussion of data, we would like to summarize the events that, in our opinion, characterize the transformation of quartz into a low friction coefficient material:

1. the tensile stress field generates fractures that open quickly, spreading over the entire volume of the area subjected to shear stress;
2. the propagation of the fractures generates the local melting of the quartz, producing the formation of amorphous silica, whose density is lower than that of the quartz; the difference in density and thermal expansion causes the fracture of the surfaces and the dispersion of the silica, which quickly solidifies in the form of nanocrystalline cristobalite (which has a marked auxetic behavior) and sometimes tridymite;
3. the accumulation of these polymorphs in the rock volumes subject to greater stress leads to a progressive reduction of friction and, easily, to the triggering of the movement.

In none of these events is the presence of water necessary.

5. Conclusions

In this work we have definitively shown that anisotropic stress on quartz crystals causes the formation of amorphous silica and, from it, at least two silica polymorphs, cristobalite and tridymite, in nanocrystalline form. These phases accumulate with the advancement of the fractures and can profoundly modify the behavior of the solid in terms of friction coefficient. Amorphous silica is, therefore, not a simple friction melting product of the surface portion of the rock subject to friction, but it is a precursor of far more complex phases that represent the memory of the event. This observation contrasts sharply with what had been hypothesized by several authors, who aim to explain the lowering of the friction coefficient of the quartz subjected to shear stress due to the simple presence of silica gel.

Given the extreme speed with which cristobalites and tridymites are formed, we can argue that these mineral phases are generated while the fracture phase is still active and that their accumulation is such as to heavily modify the rock's mechanical behavior.

Cristobalite can thus be the main cause of the collapse of the friction coefficient occurring in the friction tests on quartz and on rocks rich in quartz.

Author Contributions: Conceptualization: G.M. and P.P.; Methodology: G.M. and P.P.; Analyses and investigation: P.P., E.T., E.P.; Writing—original draft preparation: P.P.; Writing-review and editing: G.M. and P.P.; Resources and project administration: F.G. All authors have read and agreed to the published version of the manuscript.

Funding: This research received no external funding.

Acknowledgments: Thanks are due to two anonymous reviewers who contributed, with their suggestions, to improve the quality of the present paper. The Chinese Academy of Sciences Visiting Professorship partially supported Giovanni Martinelli for Senior International Scientists (2018VMA0007).

Conflicts of Interest: The authors declare no conflict of interest.

References

1. Di Toro, G.; Goldsby, D.L.; Tullis, T.E. Friction falls towards zero in quartz rock as slip velocity approaches seismic rates. *Nature* **2004**, *427*, 436–439. [CrossRef]
2. Hirose, T.; Shimamoto, T. Growth of molten zone as a mechanism of slip weakening of simulated faults in gabbro during frictional melting. *J. Geophys. Res. Space Phys.* **2005**, *110*. [CrossRef]
3. Hayashi, N.; Tsutsumi, A. Deformation textures and mechanical behavior of a hydrated amorphous silica formed along an experimentally produced fault in chert. *Geophys. Res. Lett.* **2010**, *37*, 12305. [CrossRef]
4. Nakamura, Y.; Muto, J.; Nagahama, H.; Shimizu, I.; Miura, T.; Arakawa, I. Amorphization of quartz by friction: Implication to silica-gel lubrication of fault surfaces. *Geophys. Res. Lett.* **2012**, *39*, 21303. [CrossRef]
5. Martinelli, G.; Plescia, P.; Tempesta, E. Electromagnetic emissions from quartz subjected to shear stress: Spectral signatures and geophysical implications. *Geosciences* **2020**, *10*, 140. [CrossRef]

6. Martinelli, G.; Plescia, P.; Tempesta, E. "Pre-Earthquake" Micro-Structural Effects Induced by Shear Stress on α-Quartz in Laboratory Experiments. *Geosciences* **2020**, *10*, 155. [CrossRef]
7. Tavares, L.M.; King, R.P. Single particle fracture under impact loading. *Int. J. Miner. Process.* **1998**, *54*, 1–28. [CrossRef]
8. Tavares, L.M. Optimum routes for particles breakage by impact. *Powder Technol.* **2004**, *142*, 81–91. [CrossRef]
9. Tugcam Tuzcu, E.; Rajamani, R.K. Modeling breakage rates in mills with impact energy spectra and ultra fast load cell data. *Miner. Eng.* **2011**, *24*, 252–260. [CrossRef]
10. Marcos, L.V.R.; Larruquert, J.I.; Méndez, J.A.; Aznárez, J.A. Self-consistent optical constants of SiO_2 and Ta_2O_5 films. *Opt. Mater. Express* **2016**, *6*, 3622–3637. [CrossRef]
11. Zhao, B.; Wang, J.; Coop, M.R.; Viggiani, G.; Jiang, M. An investigation of single sand particle fracture using X-ray micro-tomography. *Géotechnique* **2015**, *65*, 625–641. [CrossRef]
12. Laughner, J.W.; Newnham, R.E.; Cross, L.E. Mechanical Twinning in small quartz crystals. *Phys. Chem. Min.* **1982**, *8*, 20–24. [CrossRef]
13. Tromans, D.; Meech, J. Enhanced dissolution of minerals: Stored energy, amorphism and mechanical activation. *Miner. Eng.* **2001**, *14*, 1359–1377. [CrossRef]
14. Tromans, D.; Meech, J.A. Fracture toughness and surface energies of minerals: Theoretical estimates for oxides, sulphides, silicates and halides. *Miner. Eng.* **2002**, *15*, 1027–1041. [CrossRef]
15. Tromans, D.; Meech, J.A. Fracture toughness and surface energies of covalent minerals: Theoretical estimates. *Miner. Eng.* **2002**, *17*, 1–15. [CrossRef]
16. Richter, H. Fractography of Bioceramics. In *Key Engineering Materials*; Dusza, J., Ed.; Trans Tech Publications: Baech, Switzerland, 2003; Volume 223, pp. 157–180.
17. Weichert, R.; Shonert, K. Heat generation at the tip of a moving crack. *J. Mech. Phys. Solids* **1978**, *26*, 151–161. [CrossRef]
18. Rittel, D. On the conversion of plastic work to heat during high strain deformation of glassy polymers. *Mech. Mater.* **1999**, *31*, 131–139. [CrossRef]
19. Brodie, K.H.; Rutter, E.H. Rapid stress release caused by polymorphic transformation during the experimental deformation of quartz. *Geophys. Res. Lett.* **2000**, *27*, 3089–3092. [CrossRef]
20. Pabst, W.; Gregorova, E. Elastic Properties of silica polymorphs—A review. *Ceram. Silik.* **2013**, *57*, 167–184.
21. Yeganeh-Haeri, A.; Weidner, D.J.; Parise, J.B. Elasticity of a-Cristobalite: A Silicon Dioxide with a Negative Poisson's Ratio. *Science* **1992**, *257*, 650–652. [CrossRef] [PubMed]